

# Dalton Transactions

Accepted Manuscript



This is an *Accepted Manuscript*, which has been through the Royal Society of Chemistry peer review process and has been accepted for publication.

*Accepted Manuscripts* are published online shortly after acceptance, before technical editing, formatting and proof reading. Using this free service, authors can make their results available to the community, in citable form, before we publish the edited article. We will replace this *Accepted Manuscript* with the edited and formatted *Advance Article* as soon as it is available.

You can find more information about *Accepted Manuscripts* in the [Information for Authors](#).

Please note that technical editing may introduce minor changes to the text and/or graphics, which may alter content. The journal's standard [Terms & Conditions](#) and the [Ethical guidelines](#) still apply. In no event shall the Royal Society of Chemistry be held responsible for any errors or omissions in this *Accepted Manuscript* or any consequences arising from the use of any information it contains.

Cite this: DOI: 10.1039/c0xx00000x

www.rsc.org/xxxxxx

ARTICLE TYPE

# Halogen effects on photoluminescence and catalytic properties: a series of spatially arranged trimetallic zinc(II) complexes

Haeri Lee, Tae Hwan Noh and Ok-Sang Jung\*

Received (in XXX, XXX) Xth XXXXXXXXX 20XX, Accepted Xth XXXXXXXXX 20XX

DOI: 10.1039/b000000x

Self-assembly of  $ZnX_2$  ( $X = Cl, Br, \text{ and } I$ ) with  $N,N',N''$ -tris(2-pyridinylethyl)-1,3,5-benzenetricarboxamide (L) as a tridentate  $N$ -donor ligand yields discrete  $C_3$ -symmetric trimetallic zinc(II) complexes,  $[Zn_3X_6L(MeOH)_3]$ . These form, via  $\pi \cdots \pi$  interactions and  $NH \cdots O=C$  hydrogen-bonds, an ensemble constituting a unique columnar stacking structure in  $abab \cdots$  staggered fashion. For this series of complexes, the halogen effects on the photoluminescence, catalysis, and thermal properties were investigated. For  $[Zn_3Cl_6L(MeOH)_3]$ , a blue luminescence was observed at 462 nm ( $\lambda_{ex} = 369$  nm). The transesterification catalysis showed significant halogen effects in the order  $[Zn_3I_6L(MeOH)_3] > [Zn_3Cl_6L(MeOH)_3] > [Zn_3Br_6L(MeOH)_3]$  in methanol, whereas in a mixture of methanol and acetonitrile, the order was  $[Zn_3I_6L(MeOH)_3] > [Zn_3Br_6L(MeOH)_3] > [Zn_3Cl_6L(MeOH)_3]$ . Such notable different effects among the three complexes might be explained by the halogens' electronic effects and dissociation properties.

## Introduction

Diverse polypyridyl  $N$ -donor ligands that can coordinate two or more remote metal centers have been used to construct desirable molecular structures.<sup>1-4</sup> Current applications of such polynuclear complexes span a wide range of interesting fields such as mixed-valence species, photo-induced electron or energy transfer, magnetic exchange between paramagnetic centers, and supramolecular weak interactions.<sup>5-10</sup> Specifically, tridentate  $N$ -donor building tectonics have been employed to synthesize cage coordination complexes or  $C_3$ -symmetric triangular module metal complexes.<sup>11-18</sup> Trimetallic complexes via tridentate ligand metal ions are relatively rare, unlike the vast majority of dinuclear complexes. Unique tridentate ligands containing pyridyl moieties, for example, offer, via the introduction of appropriate metal ions, wider opportunities for trigonal metallic array. A number of such trimetallic complexes have been synthesized in recent years, especially those with a tridentate core.<sup>19</sup> Their hyper-branched structural and chemical features, with their advanced material and catalytic properties, have been a good prototype for generation of multifunctional properties.<sup>20</sup> Thus, systematic  $C_3$ -symmetric trimetallic complexes offer interesting physicochemical properties that have been found to be delicately dependent on the nature of the ligands and co-ligands.

In this context, in an investigation of the significant halogen effects of  $C_3$ -symmetric trimetallic complexes,  $ZnX_2$  ( $X = Cl, Br, \text{ and } I$ ) was reacted with  $C_3$ -symmetric  $N,N',N''$ -tris(2-pyridinylethyl)-1,3,5-benzenetricarboxamide (L).<sup>16</sup> Further to which, a systematic series of trimetallic zinc(II) complexes and their one-dimensional (1D) ensemble crystal structures formed via intermolecular forces, along with the direct halogen effects on

their photoluminescence, transesterification catalytic activity, and thermal properties, are reported herein. Zinc(II) complexes have been extensively examined for their used in appropriate tetrahedral binding Lewis acidity, metallo-enzymes, zinc finger proteins, transmetallation, and homogeneous catalysis.<sup>21-28</sup> A variety of zinc(II) coordination complexes containing aromatic moieties exhibit unique ligand-to-metal charge transfer luminescent properties that are strongly dependent on the geometry of the ligands and counteranions.<sup>23,25</sup> Furthermore, zinc(II) compounds with functional organic ligands can potentially be used in light-emitting-diode and heterogeneous-catalysis applications.<sup>22</sup>

## Experimental section

### Materials and measurements

All chemicals including zinc(II) chloride, zinc(II) bromide, zinc(II) iodide, and phenyl acetate were purchased from Aldrich, and used without further purification.  $N,N',N''$ -Tris(2-pyridinylethyl)-1,3,5-benzenetricarboxamide (L) was prepared according to the method reported in the literature.<sup>16</sup> Elemental microanalyses (C, H, N) were performed on crystalline samples at the KBSI Pusan Center using a Vario-EL III. Thermal analyses were undertaken under a nitrogen atmosphere at a scan rate of 10 °C/min using a Labsys TGA-DSC 1600. The infrared spectra of samples prepared as KBr pellets were obtained on a Nicolet 380 FT-IR spectrophotometer. The <sup>1</sup>H NMR (300MHz) spectra were recorded on a Varian Mercury Plus 300. Scanning electron microscopy (SEM) images were obtained on a Tescan VEGA 3. Powder X-ray diffraction data were recorded on a Rigaku RINT/DMAX-2500 diffractometer at 40 kV, 126 mA for Cu K $\alpha$ . Excitation and emission spectra were acquired on a FluoroMate

**Table 1** Crystallographic Data and Structure Refinement for [Zn<sub>3</sub>Cl<sub>6</sub>L(MeOH)<sub>3</sub>], [Zn<sub>3</sub>Br<sub>6</sub>L(MeOH)<sub>3</sub>], and [Zn<sub>3</sub>I<sub>6</sub>L(MeOH)<sub>3</sub>]

	[Zn <sub>3</sub> Cl <sub>6</sub> L(MeOH) <sub>3</sub> ]	[Zn <sub>3</sub> Br <sub>6</sub> L(MeOH) <sub>3</sub> ]	[Zn <sub>3</sub> I <sub>6</sub> L(MeOH) <sub>3</sub> ]
Formula	C <sub>33</sub> H <sub>42</sub> Cl <sub>6</sub> N <sub>6</sub> O <sub>6</sub> Zn <sub>3</sub>	C <sub>33</sub> H <sub>42</sub> Br <sub>6</sub> N <sub>6</sub> O <sub>6</sub> Zn <sub>3</sub>	C <sub>33</sub> H <sub>42</sub> I <sub>6</sub> N <sub>6</sub> O <sub>6</sub> Zn <sub>3</sub>
<i>M<sub>w</sub></i>	1027.54	1294.30	1576.24
Crystal system	Hexagonal	Hexagonal	Hexagonal
Space group	<i>P</i> 6 <sub>3</sub>	<i>P</i> 6 <sub>3</sub>	<i>P</i> 6 <sub>3</sub>
<i>a</i> /Å	32.1306(4)	31.5420(3)	31.9496(2)
<i>c</i> /Å	7.3880(1)	7.6862(1)	8.0211(1)
<i>V</i> /Å <sup>3</sup>	6605.3(2)	6622.5(1)	7090.8(1)
<i>Z</i>	6	6	6
$\rho$ /g cm <sup>-3</sup>	1.550	1.947	2.215
$\mu$ /mm <sup>-1</sup>	2.032	7.094	5.473
<i>F</i> (000)	3132	3780	4428
<i>R</i> <sub>int</sub>	0.0824	0.0629	0.0427
GoF on <i>F</i> <sup>2</sup>	1.064	1.115	1.188
<i>R</i> <sub>1</sub> [ <i>I</i> > 2σ( <i>I</i> )] <sup>a</sup>	0.0448	0.0419	0.0529
<i>wR</i> <sub>2</sub> (all data) <sup>b</sup>	0.1045	0.0890	0.0923

$$^a R_1 = \frac{\sum |F_o| - |F_c|}{\sum |F_o|}, \quad ^b wR_2 = \left( \frac{\sum [w(F_o^2 - F_c^2)^2]}{\sum [w(F_o^2)^2]} \right)^{1/2}$$

FS-2 spectrofluorometer. Fluorescence microscopy images were obtained with an Olympus BX51 microscope equipped with an AxioCam MRc 5 digital camera and U-MWU2 filter set.

#### Preparation of [Zn<sub>3</sub>Cl<sub>6</sub>L(MeOH)<sub>3</sub>]

A methanol solution (5 mL) of *N,N',N''*-tris(2-pyridinylethyl)-1,3,5-benzenetricarboxamide (L) (78 mg, 0.15 mmol) was added to a methanol solution (5 mL) of zinc(II) chloride (61 mg, 0.45 mmol). Slow evaporation of the solvent produced colorless crystals of [Zn<sub>3</sub>Cl<sub>6</sub>L(MeOH)<sub>3</sub>] in a 76% (117 mg) yield after 3 days. mp 300 °C (dec.). Found: C, 38.3; H, 4.2; N, 8.1. Calc. for C<sub>33</sub>H<sub>42</sub>Cl<sub>6</sub>N<sub>6</sub>O<sub>6</sub>Zn<sub>3</sub>: C, 38.6; H, 4.2; N, 8.2%. IR (KBr pellet, cm<sup>-1</sup>): 3585 (br), 3506 (br), 3367 (br), 3131 (br), 1635 (s), 1608 (s), 1548 (s), 1488 (s), 1440 (s), 1363 (m), 1307 (s), 1193 (w), 1160 (w), 1064 (w), 1024 (w), 779 (m).

#### Preparation of [Zn<sub>3</sub>Br<sub>6</sub>L(MeOH)<sub>3</sub>]

This product was prepared in the same manner as [Zn<sub>3</sub>Cl<sub>6</sub>L(MeOH)<sub>3</sub>], using ZnBr<sub>2</sub> instead of ZnCl<sub>2</sub> in a 73% (141 mg) yield. mp 303 °C (dec.). Found: C, 31.0; H, 3.2; N, 6.4. Calc. for C<sub>33</sub>H<sub>42</sub>Br<sub>6</sub>N<sub>6</sub>O<sub>6</sub>Zn<sub>3</sub>: C, 30.6; H, 3.3; N, 6.5%. IR (KBr pellet, cm<sup>-1</sup>): 3500 (br), 3363 (br), 3077 (br), 1635 (s), 1608 (s), 1542 (s), 1488 (m), 1440 (m), 1307 (m), 1159 (w), 1064 (w), 1024 (w), 775 (m).

#### Preparation of [Zn<sub>3</sub>I<sub>6</sub>L(MeOH)<sub>3</sub>]

The product also was prepared in the same manner as [Zn<sub>3</sub>Cl<sub>6</sub>L(MeOH)<sub>3</sub>], using ZnI<sub>2</sub> instead of ZnCl<sub>2</sub> in a 72% (170 mg) yield. mp 303 °C (dec.). Found: C, 25.2; H, 2.6; N, 5.3. Calc. for C<sub>33</sub>H<sub>42</sub>I<sub>6</sub>N<sub>6</sub>O<sub>6</sub>Zn<sub>3</sub>: C, 25.1; H, 2.7; N, 5.3%. IR (KBr pellet, cm<sup>-1</sup>): 3509 (br), 3378 (br), 3081 (br), 2798 (w), 1633 (s), 1608 (s), 1542 (s), 1486 (m), 1438 (m), 1307 (m), 1159 (w), 1064 (w), 1025 (w), 1002 (m), 759 (m).

#### Transesterification catalysis

Phenyl acetate (2.72 g, 2 mmol) was dissolved in methanol (15

mL) or a mixture of methanol and acetonitrile (15 mL, *v/v* = 1:1), and the catalysts (0.1 mmol; 34 mg for [Zn<sub>3</sub>Cl<sub>6</sub>L(MeOH)<sub>3</sub>]; 43 mg for [Zn<sub>3</sub>Br<sub>6</sub>L(MeOH)<sub>3</sub>]; 52 mg for [Zn<sub>3</sub>I<sub>6</sub>L(MeOH)<sub>3</sub>]) were added to the reaction solution. The reaction solution was stirred at 50 °C for both 4 h and 6 h. The reaction using [Zn<sub>3</sub>I<sub>6</sub>L(MeOH)<sub>3</sub>] was achieved at reflux temperature. The conversion yields were monitored by reference to the <sup>1</sup>H NMR spectra. All of the reactions were run at least three times and the conversion yields are averaged.

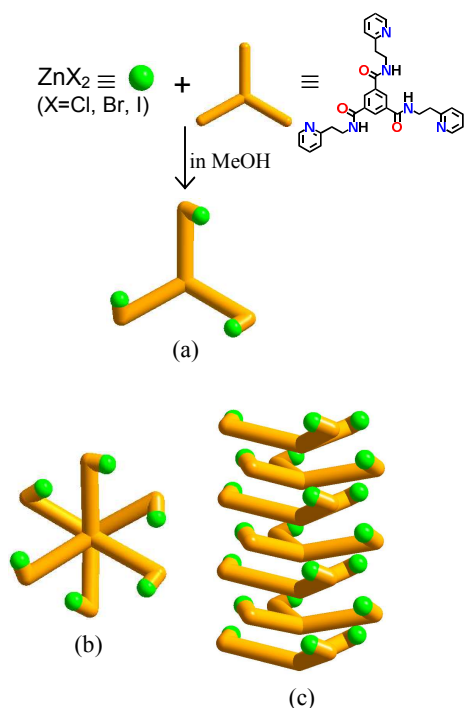
#### Crystal structure determination

X-ray data were collected on a Bruker SMART automatic diffractometer equipped with graphite-monochromated Mo *K*α radiation ( $\lambda$  = 0.71073 Å) and a CCD detector at -25 °C. Thirty-six frames of two-dimensional diffraction images were collected and processed to obtain the cell parameters and orientation matrix. The data were corrected for Lorentz and polarization effects. The absorption effects were corrected using the multi-scan method (SADABS).<sup>29</sup> The structures were solved using the direct method (SHELXS 97) and refined by full-matrix least squares techniques (SHELXL 97).<sup>30</sup> The non-hydrogen atoms were refined anisotropically, and the hydrogen atoms were placed in calculated positions and refined only for the isotropic thermal factors. The crystal parameters along with procedural information on the data collection and structure refinement are listed in Table 1.

## Result and discussion

### Synthesis

The reaction of ZnX<sub>2</sub> (X = Cl, Br, and I) with *N,N',N''*-tris(2-pyridinylethyl)-1,3,5-benzenetricarboxamide (L) as a C<sub>3</sub>-axis tridentate *N*-donor in methanol at room temperature afforded discrete C<sub>3</sub>-symmetric trimetallic zinc(II) complexes, [Zn<sub>3</sub>X<sub>6</sub>L(MeOH)<sub>3</sub>], in high yields, as shown in Scheme 1. The reactions were initially conducted in the 1 : 1 mole ratio of zinc(II) : L, but the products were not significantly affected by either the mole



**Scheme 1** Synthetic scheme of trimetallic zinc(II) complexes (a). Top view (b) and side view (c) of columnar stacking structure.

ratio or concentrations, which indicated that they were thermodynamically stable species. These products are remarkable in that there was no evidence for coordination-polymerization, not even at high concentrations, and despite the lack of protective groups. Thus, the discrete trimetallic complexes' formation might be attributable to the intrinsic properties of the reaction system. The crystalline products were not obtained in ethanol, *n*-propanol, nor *i*-propanol instead of methanol. The colorless crystalline products of  $[\text{Zn}_3\text{X}_6\text{L}(\text{MeOH})_3]$  were air-stable and dissociated in methanol, ethanol, *N,N*-dimethylformamide, and dimethyl sulfoxide, but insoluble in water, *n*-hexane, dichloromethane, chloroform, and acetone. The results of an elemental analysis and the products' NMR spectra were consistent with desirable structures.

### Crystal structures

The crystal structures of  $[\text{Zn}_3\text{X}_6\text{L}(\text{MeOH})_3]$  are basically isostructural hexagonal  $P6_3$  space groups, as depicted in Fig. 1 and S1 (see ESI†), and the relevant bond lengths and angles are listed in Table 2. Their bond lengths and angles around the zinc(II) ion differ slightly, presumably owing to the different electronic and steric effects of the halides. The local geometry around the zinc(II) ion approximates to a typical tetrahedral arrangement with two halides ( $\text{X}-\text{Zn}-\text{X} = 116.29(5)-127.00(5)^\circ$ ), a nitrogen from L, and an oxygen from the methanol molecule. The L connects three zinc(II) ions to form  $\text{C}_3$ -axis trimetallic  $[\text{Zn}_3\text{X}_6\text{L}(\text{MeOH})_3]$ . The methanol molecule acts as the fourth ligand rather than a simple solvate molecule. The intramolecular  $\text{Zn}\cdots\text{Zn}$  distances of  $[\text{Zn}_3\text{Cl}_6\text{L}(\text{MeOH})_3]$ ,  $[\text{Zn}_3\text{Br}_6\text{L}(\text{MeOH})_3]$ , and  $[\text{Zn}_3\text{I}_6\text{L}(\text{MeOH})_3]$  are 11.981(3)–12.0573(8) Å, 12.304(1)–12.521(1) Å, and 12.509(2)–12.675(2) Å, respectively. Intramolecular interactions of  $\text{MeOH}\cdots\text{O}=\text{C}$  (1.78–1.79 Å for  $[\text{Zn}_3\text{Cl}_6\text{L}(\text{MeOH})_3]$ ; 1.81–1.85 Å for  $[\text{Zn}_3\text{Br}_6\text{L}(\text{MeOH})_3]$ ; 1.74–1.91 Å for  $[\text{Zn}_3\text{I}_6\text{L}(\text{MeOH})_3]$ )

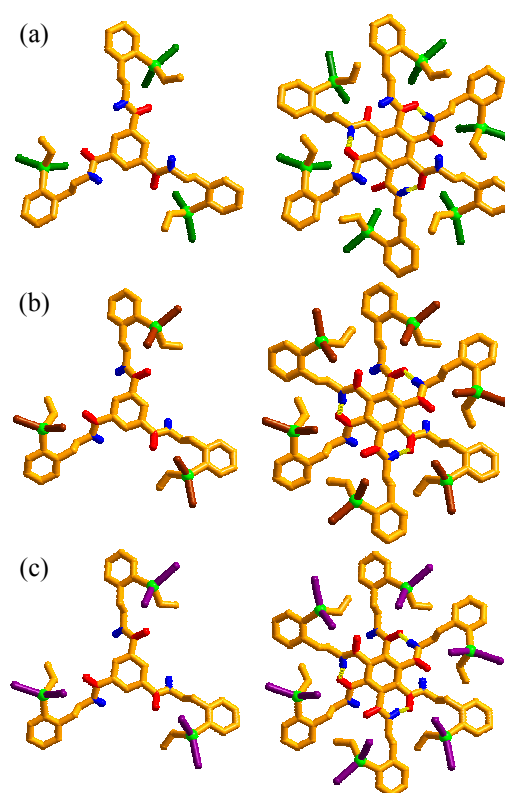


**Fig. 1** Top views of single (left) and double (right) molecules of  $[\text{Zn}_3\text{X}_6\text{L}(\text{MeOH})_3]$  (a),  $[\text{Zn}_3\text{Br}_6\text{L}(\text{MeOH})_3]$  (b), and  $[\text{Zn}_3\text{I}_6\text{L}(\text{MeOH})_3]$  (c).

$\text{L}(\text{MeOH})_3]$  exist in the solid state (Fig. 1). All of the products showed an infinite 1D column ensemble via close intermolecular  $\pi\cdots\pi$  contacts (3.6839(5)–3.7041(5) Å for  $[\text{Zn}_3\text{Cl}_6\text{L}(\text{MeOH})_3]$ ; 3.83(4)–3.86(4) Å for  $[\text{Zn}_3\text{Br}_6\text{L}(\text{MeOH})_3]$ ; 3.954(4)–4.011(4) Å for  $[\text{Zn}_3\text{I}_6\text{L}(\text{MeOH})_3]$ ) and intermolecular hydrogen-bondings (2.21–2.25 Å or  $[\text{Zn}_3\text{Cl}_6\text{L}(\text{MeOH})_3]$ ; 2.30–2.39 Å for  $[\text{Zn}_3\text{Br}_6\text{L}(\text{MeOH})_3]$ ; 2.36–2.69 Å for  $[\text{Zn}_3\text{I}_6\text{L}(\text{MeOH})_3]$ ) between  $\text{NH}\cdots\text{O}=\text{C}$  in an *abab* layer (Fig. 2). The  $\pi\cdots\pi$  interactions and hydrogen-bondings were comparable to the results reported by Valencia *et al.*<sup>31</sup> and Jung *et al.*,<sup>15</sup> respectively. The columns were arranged in a hexagonal packing mode, as depicted in Fig. 3. Thus, the slightly different bond lengths and angles showed significant halogen effects. No other exceptional features, neither with respect to bond lengths nor to angles, were observed. The three tetrahedral zinc(II) moieties are in a propeller-like arrangement in the same upside direction from the central benzene. Accordingly,  $[\text{Zn}_3\text{Br}_6\text{L}(\text{MeOH})_3]$  and  $[\text{Zn}_3\text{I}_6\text{L}(\text{MeOH})_3]$  are chiral crystalline solids consisting of two-column *P*-helices and one-column *M*-helices (where *P* denoted right-handed helices and *M* denotes left-handed helices), whereas  $[\text{Zn}_3\text{Cl}_6\text{L}(\text{MeOH})_3]$  is a crystalline solid consisting of one-column *P*-helices and two-column *M*-helices. All of the crystals in the reaction vessel were a mixture of chiral crystals and enantiomeric crystals.

### Construction principle

By the reaction of  $\text{ZnX}_2$  with L in methanol, discrete  $\text{C}_3$ -symmetric trimetallic zinc(II) complexes,  $[\text{Zn}_3\text{X}_6\text{L}(\text{MeOH})_3]$ , not coordination polymeric species, were obtained in high yields. The present complexes were favorably formed irrespective of concentrations or mole ratios, indicating the thermodynamically

**Table 2** Selected Bond Distances (Å) and Bond Angles (°) for  $[\text{Zn}_3\text{Cl}_6\text{L}(\text{MeOH})_3]$ ,  $[\text{Zn}_3\text{Br}_6\text{L}(\text{MeOH})_3]$ , and  $[\text{Zn}_3\text{I}_6\text{L}(\text{MeOH})_3]$ 

	$[\text{Zn}_3\text{Cl}_6\text{L}(\text{MeOH})_3]$	$[\text{Zn}_3\text{Br}_6\text{L}(\text{MeOH})_3]$	$[\text{Zn}_3\text{I}_6\text{L}(\text{MeOH})_3]$
Zn(1)–N(1)	2.061(3)	2.043(5)	2.044(7)
Zn(1)–O(2)	1.988(3)	2.050(5)	2.052(6)
Zn(1)–X(1)	2.199(1)	2.338(1)	2.569(1)
Zn(1)–X(2)	2.229(1)	2.368(1)	2.529(1)
Zn(2)–N(3)	2.121(4)	2.040(4)	2.058(7)
Zn(2)–O(4)	2.018(4)	2.044(5)	2.032(7)
Zn(2)–X(3)	2.225(2)	2.3419(8)	2.577(1)
Zn(2)–X(4)	2.179(2)	2.3729(9)	2.523(1)
Zn(3)–N(5)	2.053(3)	2.036(4)	2.042(7)
Zn(3)–O(6)	2.015(3)	2.053(5)	2.026(6)
Zn(3)–X(5)	2.194(1)	2.3398(8)	2.536(1)
Zn(3)–X(6)	2.225(1)	2.3769(9)	2.578(1)
N(1)–Zn(1)–O(2)	110.2(1)	112.8(2)	103.1(3)
N(1)–Zn(1)–X(1)	110.1(1)	107.0(2)	112.8(2)
N(1)–Zn(1)–X(2)	109.0(1)	108.5(2)	112.5(2)
X(1)–Zn(1)–X(2)	118.7(5)	127.00(5)	116.29(5)
N(3)–Zn(2)–O(4)	107.8(2)	106.2(2)	111.2(3)
N(3)–Zn(2)–X(3)	110.7(1)	110.32(1)	104.9(2)
N(3)–Zn(2)–X(4)	109.0(1)	112.5(1)	111.5(2)
X(3)–Zn(2)–X(4)	120.1(9)	118.80(4)	124.38(5)
N(5)–Zn(3)–O(6)	107.8(1)	102.5(2)	100.2(3)
N(5)–Zn(3)–X(5)	108.93(9)	111.9(1)	112.9(2)
N(5)–Zn(3)–X(6)	110.61(9)	112.8(1)	114.6(2)
X(5)–Zn(3)–X(6)	120.84(5)	118.59(4)	116.90(5)

stability of their skeletal structures. However, as noted already in the “Synthesis” section above, solvent is an important factor in the formation of trimetallic complex crystals. What is the critical driving force behind the formation of the discrete trimetallic complexes rather than coordination polymers? A combination of tetrahedral zinc(II) ions and the appropriate tridentate *N*-donors seems to be dispositive. Specifically, formation might be attributable to the *ortho*-pyridyl *N*-donor of L. That is, such an *N*-donor might be an obstacle to the formation of coordination polymers. Moreover, intramolecular hydrogen-bonding between  $\text{MeOH}\cdots\text{O}=\text{C}$  perhaps partially contributes to the formation of discrete trimetallic species. This would explain the key role of methanol in the self-assembly system. Another important feature is that both the intermolecular  $\text{NH}\cdots\text{O}=\text{C}$  hydrogen-bonds and the  $\pi\cdots\pi$  interactions can be attributed to the formation of the thermodynamically stable columnar *abab*···staggered stacking ensemble. As the present system did not reveal significant angle strains, we considered the formation of the overall crystalline structure to be due in part to the felicitous “weak interactions” rather than to the characteristics of the “geometry around the zinc(II) ion”.

### Photoluminescence

Great attention recently has been paid to  $d^{10}$  metal complexes, given their variety of applications in chemical sensors, photochemistry, and electroluminescent display.<sup>32</sup> The excitation and emission spectra of the present zinc(II) complexes then,

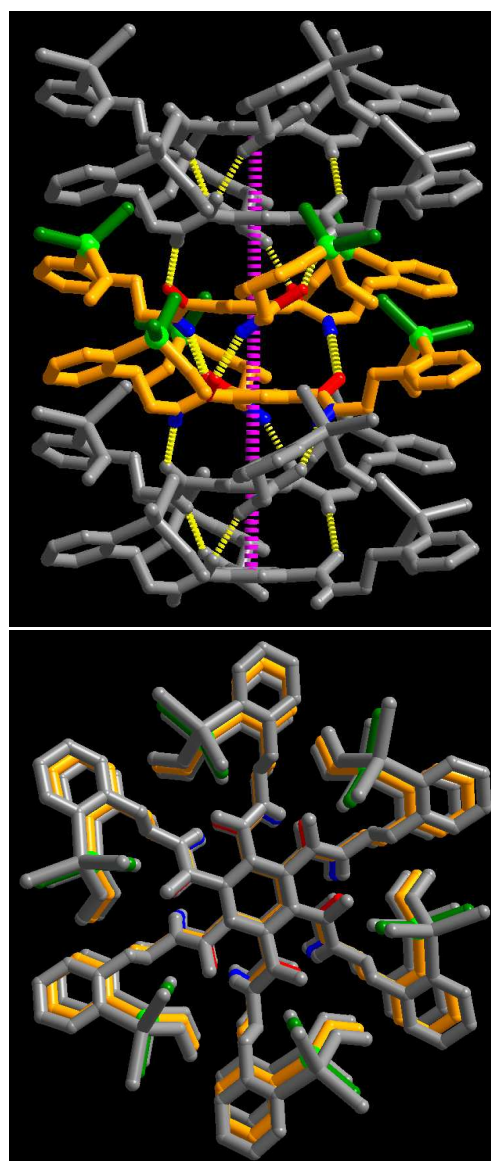


**Fig. 2** Side view (top) and top view (bottom) of columnar  $[\text{Zn}_3\text{Cl}_6\text{L}(\text{MeOH})_3]$ . The pink and yellow dashed lines denote the intermolecular  $\pi\cdots\pi$  interactions and  $\text{NH}\cdots\text{O}=\text{C}$  hydrogen-bonds, respectively.

together with those of L, were measured in the solid state at room temperature (Figs. 4 and S2, see ESI†). Emissions were observed at 462 nm ( $\lambda_{\text{ex}} = 421$  nm) for  $[\text{Zn}_3\text{Cl}_6\text{L}(\text{MeOH})_3]$ , 466 nm ( $\lambda_{\text{ex}} = 401$  nm) for  $[\text{Zn}_3\text{Br}_6\text{L}(\text{MeOH})_3]$ , and 482 nm ( $\lambda_{\text{ex}} = 372$  nm) for  $[\text{Zn}_3\text{I}_6\text{L}(\text{MeOH})_3]$ . The emission bands of  $[\text{Zn}_3\text{Cl}_6\text{L}(\text{MeOH})_3]$  and  $[\text{Zn}_3\text{Br}_6\text{L}(\text{MeOH})_3]$  were blue-shifted relative to the corresponding ligand L ( $\lambda_{\text{em}} = 480$  nm;  $\lambda_{\text{ex}} = 421$  nm), while  $[\text{Zn}_3\text{I}_6\text{L}(\text{MeOH})_3]$  was red-shifted. The ligand’s intrinsic characteristics play a pivotal role in the photoluminescence mechanism of the present zinc(II) complexes. These results suggest that the complexes’ emission bands can be ascribed to the ligand-to-metal charge transfer (LMCT).<sup>33,34</sup> The red-shift from  $[\text{Zn}_3\text{Cl}_6\text{L}(\text{MeOH})_3]$  to  $[\text{Zn}_3\text{I}_6\text{L}(\text{MeOH})_3]$  can be explained by the electronic effects of halides and the coordination environments of the zinc(II) ions.<sup>35–37</sup> And it is worthwhile, additionally, to mention that  $[\text{Zn}_3\text{Cl}_6\text{L}(\text{MeOH})_3]$  showed much stronger emissions than those of  $[\text{Zn}_3\text{Br}_6\text{L}(\text{MeOH})_3]$  and  $[\text{Zn}_3\text{I}_6\text{L}(\text{MeOH})_3]$  at room temperature.

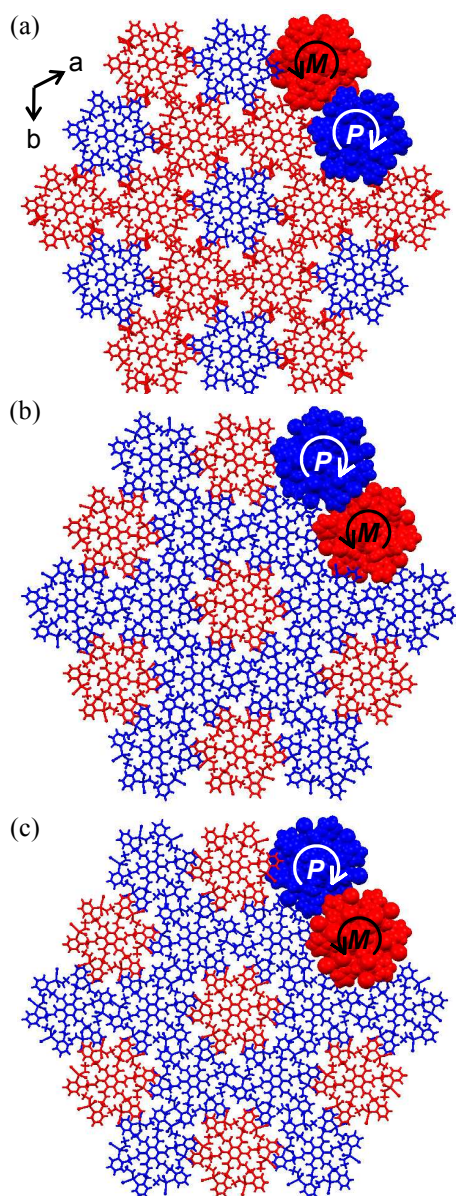


**Fig. 3** Packing diagrams of  $[\text{Zn}_3\text{Cl}_6\text{L}(\text{MeOH})_3]$  (a),  $[\text{Zn}_3\text{Br}_6\text{L}(\text{MeOH})_3]$  (b), and  $[\text{Zn}_3\text{I}_6\text{L}(\text{MeOH})_3]$  (c). Red: *M*-helical column; blue: *P*-helical column.

Such a significant difference can be attributed to the effective increase of the Zn–Cl bond rigidity and the reduction in the loss of energy through radiation-less decay. However, the quantum yield of  $[\text{Zn}_3\text{Cl}_6\text{L}(\text{MeOH})_3]$  (0.084%) is lower than that of the known iridium(III) complex, FIrpic (0.42%).<sup>38</sup> In order to achieve, via the inter-molecular  $\text{NH}\cdots\text{O}=\text{C}$  hydrogen-bonds and the  $\pi\cdots\pi$  interaction, the ensemble effect on the photoluminescence, their solution spectra were attempted in  $\text{Me}_2\text{SO}$ , resulting in partial dissociation (see ESI†).

### 10 Transesterification catalysis

In order to investigate the halogen effects on the catalytic reactions, the  $[\text{Zn}_3\text{X}_6\text{L}(\text{MeOH})_3]$  series have been employed as a homogeneous catalyst of the transesterification reaction of phenyl acetate with methanol. Various catalysts available for transesteri-

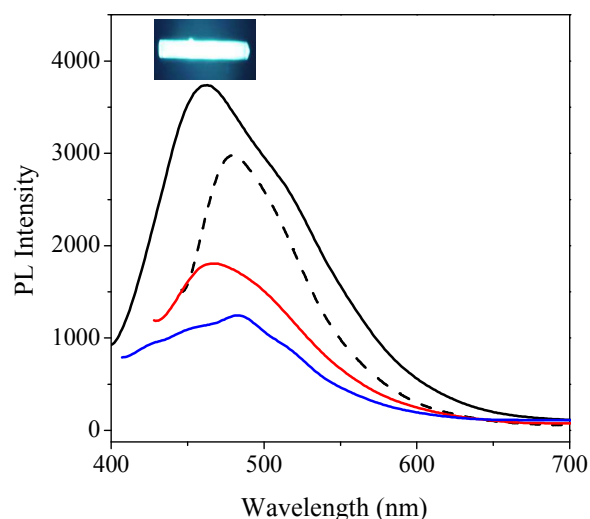


**Fig. 4** Solid-state photoluminescence spectra of L (dashed line),  $[\text{Zn}_3\text{Cl}_6\text{L}(\text{MeOH})_3]$  (black solid line),  $[\text{Zn}_3\text{Br}_6\text{L}(\text{MeOH})_3]$  (red solid line), and  $[\text{Zn}_3\text{I}_6\text{L}(\text{MeOH})_3]$  (blue solid line) at room temperature. Inset: fluorescent-microscopic image of  $[\text{Zn}_3\text{Cl}_6\text{L}(\text{MeOH})_3]$ .

15 fication of a wide range of esters with alcohol under mild conditions have been developed.<sup>27,28</sup> In the present investigation,  $[\text{Zn}_3\text{X}_6\text{L}(\text{MeOH})_3]$  ( $\text{X} = \text{Cl}, \text{Br}, \text{and I}$ ) (0.1 mmol) significantly catalyzed the transesterification of phenyl acetate (2 mmol) with an excess amount of methanol at 50 °C for 4 h or 6 h, as depicted  
20 in Fig. 5. A control reaction without the catalysts, meanwhile, showed trace amounts of ester-converted product. Another catalytic reaction with authentic  $\text{ZnI}_2$  exhibited the 13.8% conversion yield at 50 °C for 6 h. The catalysis process was monitored by reference to the  $^1\text{H}$  NMR spectra (see ESI†). The  
25 trimetallic zinc(II) complexes showed, on catalytic activity in methanol, significant halogen effects in the order  $[\text{Zn}_3\text{I}_6\text{L}(\text{MeOH})_3] > [\text{Zn}_3\text{Cl}_6\text{L}(\text{MeOH})_3] > [\text{Zn}_3\text{Br}_6\text{L}(\text{MeOH})_3]$ . The coordinated (activated) methanol molecule might be a key factor in transesterification. Of course, the 6 h catalysis showed a  
30 higher conversion than that of 4 h. It seems that the catalytic effects, as plotted for the present case in Fig. 5, are strongly dependent on the dissociation of the Zn–X bonds. It is not easy to elucidate the exact mechanism of catalysis at this stage, though the mechanism of metal-ion-catalyzed transesterification  
35 probably involves electrophilic activation of the carbon center of the carbonyl moiety by binding of the metal to the carbonyl oxygen.<sup>28</sup> If so, vacant site and the Lewis acidity of the zinc metal center, accordingly, play important roles in this catalytic reaction. Thus, the process of leaving group's dissociation seems to be one  
40 of the conversion-rate-determining steps. And if this is the case, the catalysis reaction will show significant solvent effects. Therefore, in the present study, the catalysis reaction was carried out in a mixture of methanol and acetonitrile instead of (only) methanol; the resulting the activity order was  $[\text{Zn}_3\text{I}_6\text{L}(\text{MeOH})_3] >$   
45  $[\text{Zn}_3\text{Br}_6\text{L}(\text{MeOH})_3] > [\text{Zn}_3\text{Cl}_6\text{L}(\text{MeOH})_3]$ . That is,  $[\text{Zn}_3\text{I}_6\text{L}(\text{MeOH})_3]$  and  $[\text{Zn}_3\text{Br}_6\text{L}(\text{MeOH})_3]$  showed high activity in the mixture solvent whereas  $[\text{Zn}_3\text{Cl}_6\text{L}(\text{MeOH})_3]$  demonstrated high activity in the methanol. This result suggests that Zn–Cl is less dissociated in the mixture solvent than in methanol whereas Zn–I and Zn–Br  
50 are more dissociated in the mixture solvent than in methanol. The

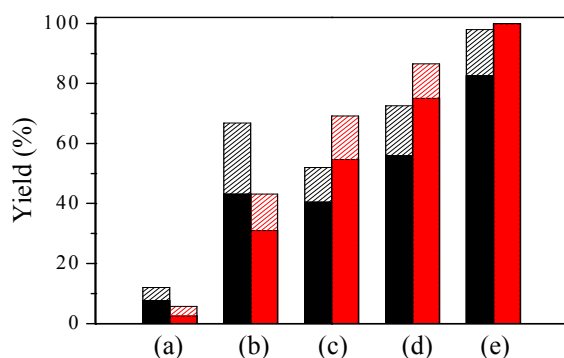


**Fig. 5** Transesterification of phenyl acetate by methanol without catalyst (a), in presence of  $[\text{Zn}_3\text{Cl}_6\text{L}(\text{MeOH})_3]$  (b),  $[\text{Zn}_3\text{Br}_6\text{L}(\text{MeOH})_3]$  (c), and  $[\text{Zn}_3\text{I}_6\text{L}(\text{MeOH})_3]$  (d) all at 50 °C, and in presence of  $[\text{Zn}_3\text{I}_6\text{L}(\text{MeOH})_3]$  at reflux temperature (e). Black column: catalysis in methanol; red column: mixture of methanol and acetonitrile ( $v/v = 1 : 1$ ); filled: catalysis for 4 h; dashed: catalysis for 6 h.

catalysis showed significant halogen effects both for the activity with respect to the solvent. With  $[\text{Zn}_3\text{I}_6\text{L}(\text{MeOH})_3]$ , the 4 h reflux-temperature catalytic reaction in the mixture solvent effected complete conversion.

### 5 Thermal properties

The thermogravimetric analysis results for  $[\text{Zn}_3\text{X}_6\text{L}(\text{MeOH})_3]$  are plotted in Fig. 6. As can be seen, the skeletal structure was stable up to 300 °C before collapsing within the 300–550 °C range. The high collapse temperature can be attributed to the angle-strain-free structure. The coordinated methanol molecules began to evaporate at 104 °C (weight loss found: 9.2%; calcd: 9.4%) for  $[\text{Zn}_3\text{Cl}_6\text{L}(\text{MeOH})_3]$ , at 162 °C (found: 8.8%; calcd: 7.4%) for  $[\text{Zn}_3\text{Br}_6\text{L}(\text{MeOH})_3]$ , and at 171 °C (found: 6.2%; calcd: 6.1%) for  $[\text{Zn}_3\text{I}_6\text{L}(\text{MeOH})_3]$ . This triggered significant halogen effects. In order to confirm the morphology change of the crystals during the skeletal collapse, all of the crystalline samples were monitored by SEM. It was found that all of the crystals ultimately had changed to zinc(II) oxide crystals, but that their morphologies differed according to the halogens. Images of the zinc(II) oxide crystals are provided in Fig. 6. Calcination for 1, 1, and 4 h at 200, 400, and 600 °C, respectively, effected contraction via eruption of both coordinated and burned organic molecules, thus producing the characteristic morphologies (see ESI†). The SEM images revealed that for  $[\text{Zn}_3\text{I}_6\text{L}(\text{MeOH})_3]$ , the complex melted after the 200 °C calcination, and that at 400 °C, the compound changed to zinc(II) oxide micro-crystals of 1–5 μm size, which fact was confirmed by SEM-EDS; finally, at 600 °C, differently shaped zinc(II) oxide submicro-crystals formed. These results established that this method is an efficient means of morphological control of zinc(II) oxide crystals via structural difference. According to the SEM-EDS and powder X-ray diffraction pattern results, the final crystalline solids consisted of zinc(II) oxide. Zinc(II) oxide is widely used as an additive in numerous materials and products including plastics, ceramics, glass, cement, lubricants, paints, ointments, adhesives, sealants, pigments, foods (zinc-nutrient sources), batteries, ferrites, fire retardants, and first aid bandages. In materials science, different morphologies of zinc(II) oxide crystals serve task-specific functions such as in wide-band gap semiconductors of good transparency, high electron mobility, and strong room-temperature luminescence.<sup>39</sup>

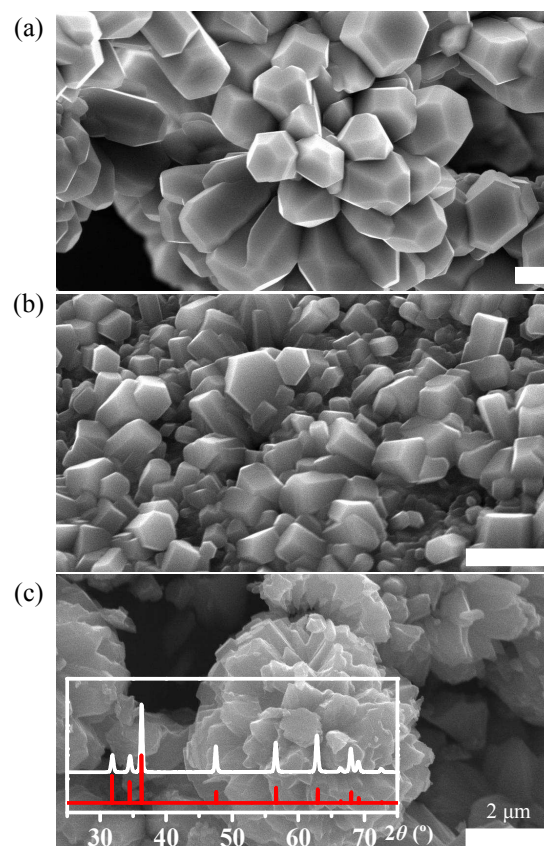
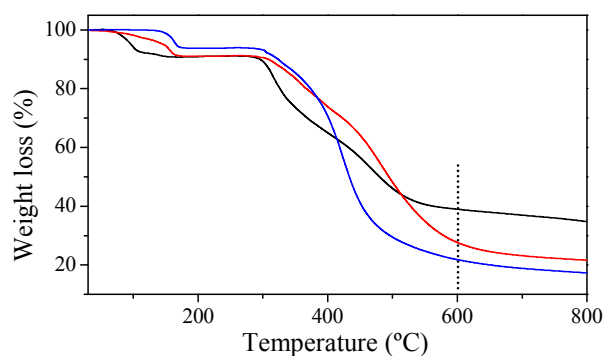


**Fig. 6** Top: TGA curves of  $[\text{Zn}_3\text{Cl}_6\text{L}(\text{MeOH})_3]$  (black),  $[\text{Zn}_3\text{Br}_6\text{L}(\text{MeOH})_3]$  (red), and  $[\text{Zn}_3\text{I}_6\text{L}(\text{MeOH})_3]$  (blue); bottom: morphologies of the residues of  $[\text{Zn}_3\text{Cl}_6\text{L}(\text{MeOH})_3]$  (a),  $[\text{Zn}_3\text{Br}_6\text{L}(\text{MeOH})_3]$  (b), and  $[\text{Zn}_3\text{I}_6\text{L}(\text{MeOH})_3]$  (c) after calcination at 600 °C for 4 h. Inset: powder XRD data for zinc(II) oxide residue (white) and reference pattern (red) from ICDD database (PDF no. 36-1451).

### Conclusions

Reaction of zinc(II) halides with a  $C_3$ -symmetric tridentate  $N$ -donor ligand afforded  $C_3$ -symmetric trimetallic zinc(II) complexes. This system appears to represent an important conceptual advance in the development of new discrete symmetric trimetallic complexes, not coordination polymers, via unique inter- and intra-molecular interactions.

Their photoluminescence properties show significant halogen effects, and  $[\text{Zn}_3\text{Cl}_6\text{L}(\text{MeOH})_3]$  particularly, shows a blue emission. These compounds are potential candidates for incorporation into luminescent sensors and photoactive materials (e.g., for

detection of aromatic organic molecules). This catalysis work reveals that both direct halogen effects and solvent systems play very important roles in transesterification. Calcination of the materials results in formation of different morphologies of zinc(II) oxide. More systematic studies, for example on the synthesis of related ligands, are in progress. Further experiments, moreover, will provide more detailed information on the enormous potentials of the complexes' catalytic properties and photoluminescence.

## Acknowledgements

This work was supported by a National Research Foundation of Korea (NRF) grant funded by the Korean Government [MEST] (2013-067841).

## Notes and references

- 15 *Department of Chemistry, Pusan National University, Pusan 609-735, Korea. Fax: 82 51 516 7421; Tel: 82 51 510 2591; E-mail: oksjung@pusan.ac.kr*
- † Electronic Supplementary Information (ESI) available: the distances of weak inter- and intra-molecular interactions, ORTEP images, solid-state excitation spectra, photoluminescence spectra in Me<sub>2</sub>SO of [Zn<sub>3</sub>Cl<sub>6</sub>L(MeOH)<sub>3</sub>], [Zn<sub>3</sub>Br<sub>6</sub>L(MeOH)<sub>3</sub>], and [Zn<sub>3</sub>I<sub>6</sub>L(MeOH)<sub>3</sub>]; partial <sup>1</sup>H NMR spectra showing catalytic effects for transesterification of phenyl acetate using [Zn<sub>3</sub>I<sub>6</sub>L(MeOH)<sub>3</sub>]; SEM images of calcined [Zn<sub>3</sub>I<sub>6</sub>L(MeOH)<sub>3</sub>] at 200 °C for 1 h, 400 °C for 1 h. CCDC 970293-970295. See DOI: 10.1039/b000000x/
- 1 E. C. Constable, *Tetrahedron*, 1992, **48**, 10013-10059.
  - 2 N. B. Debata, D. Tripathy and D. K. Chand, *Coord. Chem. Rev.*, 2012, **256**, 1831-1945.
  - 3 R. Chakrabarty, P. S. Mukherjee and P. J. Stang, *Chem. Rev.*, 2011, **111**, 6810-6918.
  - 4 W. L. Leong and J. J. Vittal, *Chem. Rev.*, 2011, **111**, 688-764.
  - 5 C. Janiak, *Dalton Trans.*, 2003, 2781-2804.
  - 6 N. G. R. Hearn, J. L. Koecok, M. M. Paquette and K. E. Preuss, *Inorg. Chem.*, 2006, **45**, 8817-8819.
  - 7 M. Grazel, *Inorg. Chem.*, 2005, **44**, 6841-6851.
  - 8 V. J. Catalano, W. E. Larson, M. M. Olmstead and H. B. Gray, *Inorg. Chem.*, 1994, **33**, 4502-4509.
  - 9 A. I. Baba, H. E. Ensley and R. H. Schmehl, *Inorg. Chem.*, 1995, **34**, 1198-1207.
  - 10 A. J. Amoroso, A. M. W. C. Thomson, J. P. Maher, J. A. McCleverty and M. D. Ward, *Inorg. Chem.*, 1995, **34**, 4828-4835.
  - 11 T. H. Noh, E. Heo, K. H. Park and O.-S. Jung, *J. Am. Chem. Soc.*, 2011, **133**, 1236-1239.
  - 12 M. Fujita, N. Fujita, K. Ogura and K. Yamaguchi, *Nature*, 1999, **400**, 52-55.
  - 13 S. Ghosh and P. S. Mukherjee, *J. Org. Chem.*, 2006, **71**, 8412-8416.
  - 14 D. Moon, S. Kang, J. Park, K. Lee, R. P. John, H. Won, G. H. Seong, Y. S. Kim, H. Rhee and M. S. Lah, *J. Am. Chem. Soc.*, 2006, **128**, 3530-3531.
  - 15 H. Lee, T. H. Noh and O.-S. Jung, *Angew. Chem., Int. Ed.*, 2013, **52**, 11790-11795.
  - 16 H. Lee, T. H. Noh and O.-S. Jung, *CrystEngComm*, 2013, **15**, 1832-1835.
  - 17 W. Hong, H. Lee, T. H. Noh and O.-S. Jung, *Dalton Trans.*, 2013, **42**, 11092-11099.
  - 18 S. Hasegawa, S. Horike, R. Matsuda, S. Furukawa, K. Mochizuki, Y. Kinoshita and S. Kitagawa, *J. Am. Chem. Soc.*, 2007, **129**, 2607-2614.
  - 19 H. Xia, T. B. Wen, Q. Y. Hu, X. Wang, X. Chen, L. Y. Shek, I. D. Williams, K. S. Wong and G. Jia, *Organometallics*, 2005, **24**, 562-569.
  - 20 N. J. Long and C. K. Williams, *Angew. Chem., Int. Ed.*, 2003, **42**, 2586-2617.
  - 21 A. W. Kleij, M. Kuil, D. M. Tooke, M. Lutz, A. L. Spek and J. N. H. Reek, *Chem. Eur. J.*, 2005, **11**, 4743-4750.
  - 22 J. W. Shin, J. M. Bae, C. Kim and K. S. Min, *Inorg. Chem.*, 2013, **52**, 2265-2267.
  - 23 S. P. Jang, J. I. Poong, S. H. Kim, T. G. Lee, J. Y. Noh and C. Kim, *Polyhedron*, 2012, **33**, 194-202.
  - 24 S. Enthaler, *ACS Catal.*, 2013, **3**, 150-158.
  - 25 T. M. McCormick and S. Wang, *Inorg. Chem.*, 2008, **47**, 10017-10024.
  - 26 W. N. Lipscomb and N. Strater, *Chem. Rev.*, 1996, **96**, 2375-2434.
  - 27 C. A. Grapperhaus, T. Tuntulani, J. H. Reibenspies and M. Y. Darensbourg, *Inorg. Chem.*, 1998, **37**, 4052-4058.
  - 28 L. S. Felices, E. C. Escudero-Adan, J. Benet-Buchholz and A. W. Kleij, *Inorg. Chem.*, 2009, **48**, 846-853.
  - 29 G. M. Sheldrick, *SADABS, A Program for Empirical Absorption Correction of Area Detector Data*, University of Göttingen: Germany, 1996.
  - 30 G. M. Sheldrick, *SHELXS-97: A Program for Structure Determination*, University of Göttingen: Germany, 1997; G. M. Sheldrick, *SHELXL-97: A Program for Structure Refinement*, University of Göttingen: Germany, 1997.
  - 31 L. Valencia, P. Pérez-Lourido, R. Bastida and A. Macías, *Cryst. Growth Des.*, 2008, **8**, 2080-2082.
  - 32 P. Jiang and Z. Guo, *Coord. Chem. Rev.*, 2004, **248**, 205-229.
  - 33 B. Valeur, in *Molecular Fluorescence: Principles and Applications*, Wiley-VCH: Weinheim, 2002.
  - 34 S. L. Zheng, M. L. Tong and X. M. Chen, *J. Chem. Soc., Dalton Trans.*, 2001, 586-592.
  - 35 J. Luo, W. S. Li, P. Xu, L. Y. Zhang and Z. N. Chen, *Inorg. Chem.*, 2012, **51**, 9508-9516.
  - 36 H. Kunkely and A. Vogler, *Chem. Phys. Lett.*, 2003, **376**, 226-229.
  - 37 A. Horváth, C. E. Wood and K. L. Stevenson, *J. Phys. Chem.*, 1994, **98**, 6490-6495.
  - 38 C. Adachi, R. C. Kwong, P. Djurovich, V. Adamovich, M. A. Baldo, M. E. Thompson and S. R. Forrest, *Appl. Phys. Lett.*, 2001, **79**, 2082-2084.
  - 39 A. Hernandezbattez, R. Gonzalez, J. Viesca, J. Fernandez, J. Diazfernandez, A. MacHado, R. Chou and J. Riba, *Wear*, 2008, **265**, 422-428.

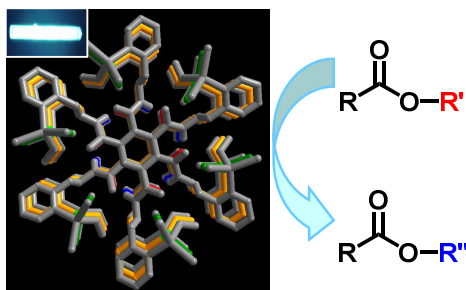


&lt;Table of Contents&gt;

## Halogen effects on photoluminescence and catalytic properties: a series of spatially arranged trimetallic zinc(II) complexes

Haeri Lee, Tae Hwan Noh and Ok-Sang Jung\*

*Department of Chemistry, Pusan National University, Pusan 609-735, Korea*



Halogen effects of a unique columnar ensemble of discrete trimetallic zinc(II) complexes formed via  $\pi\cdots\pi$  interactions and hydrogen-bonds were investigated.